Title: The role of the anterior insula in social norm compliance
and enforcement: evidence from coordinate-based and
functional connectivity meta-analyses

Authors: Gabriele Bellucci, Chunliang Feng, Julia Camilleri,
Simon B. Eickhoff, Frank Krueger

PII: S0149-7634(17)30833-3
DOI: https://doi.org/10.1016/j.neubiorev.2018.06.024
Reference: NBR 3167

To appear in:

Received date: 12-11-2017
Revised date: 29-3-2018
Accepted date: 25-6-2018

Please cite this article as: Bellucci G, Feng C, Camilleri J, Eickhoff SB, Krueger F, The role of the anterior insula in social norm compliance and enforcement: evidence from coordinate-based and functional connectivity meta-analyses, *Neuroscience and Biobehavioral Reviews* (2018), https://doi.org/10.1016/j.neubiorev.2018.06.024

Title

The role of the anterior insula in social norm compliance and enforcement: evidence from coordinate-based and functional connectivity meta-analyses

Abbreviated title

Role of the anterior insula in norm compliance and enforcement

Author names and affiliations

Gabriele Bellucci [1†], Chunliang Feng [2,3†], Julia Camilleri [4,5], Simon B. Eickhoff [4,5], Frank Krueger [6,7*]

[1] Department of Psychology, University of Lübeck, Germany

[2] State Key Laboratory of Cognitive Neuroscience and Learning, Beijing Normal University, China

[3] College of Information Science and Technology, Beijing Normal University, China

[4] Institute of Neuroscience and Medicine, Brain & Behaviour (INM-7), Research Center Jülich, Jülich, Germany

[5] Institute for Systems Neuroscience, Medical Faculty, Heinrich-Heine University Düsseldorf, Germany

[6] School of Systems Biology, George Mason University, Fairfax, VA, USA

[7] Department of Psychology, University of Mannheim, Mannheim, Germany

[†] G.B. and C.F. contributed equally to this work

*Corresponding author

Frank Krueger, Ph.D.

School of Systems Biology

George Mason University

Fairfax, VA, 22030 USA

FKrueger@gmu.edu

Manuscript Information

Number of pages: *24*

Number of figures and tables: *4/4*

Number of words for Abstract/Introduction/Discussion: *171/1,481/1,917*

Number of Supplementary Tables: *5*

Research Highlights

- Different anterior insula (AI) regions underlie social behaviors in economic games
- Dorsal AI activation is related to expectancy of norm compliance
- Ventral AI is associated with negative feelings motivating norm enforcement

Abstract

Economic games —trust (TG) and ultimatum game (UG)— combined with fMRI have shown the importance of the anterior insula (AI) in social normative behaviors. However, whether different AI subregions are engaged in different cognitive and affective processes for social norm compliance and norm enforcement during social exchange remains elusive. Here, we investigated the role of the dorsal AI (dAI) and ventral AI (vAI), combining a coordinate-based meta-analysis of fMRI studies using the TG and UG with meta-analytic task-based and task-free connectivity analyses. Our findings showed that the right dAI and vAI were the only common brain regions consistently activated across games. These clusters were part of two functionally distinguishable connectivity networks associated with cognitive (dAI) and emotional (vAI) processes. In conclusion, we propose that dAI mediates cognitive processes that generate expectancy for norm compliance, whereas vAI mediates aversive feelings that generate motivation to norm enforcement. The identified functional differentiation of the right AI in the social domain contributes to a better understanding of its role in basic and clinical neuroscience.

Key words: trust game, ultimatum game, norm compliance, norm enforcement, inequity aversion, activation likelihood estimation, meta-analytic connectivity mapping, resting-state functional connectivity

Introduction

Human societies need prescriptions and proscriptions for their members to successfully interact with each other. *Social norms* represent a fundamental grammar of social interaction and refer to behaviors collectively approved or disapproved in a group (Bicchieri, 2005). As a "cluster of expectations", they allow individuals to anticipate others' behaviors and to adopt expected behaviors (Bicchieri, 1990, 2014). Social norms (e.g., fairness, reciprocity) promote equal resource distributions and stabilize cooperation with better collective solutions than those attained by the single, self-interested individuals (Buckholtz and Marois, 2012). Group prosperity is enhanced if all members comply with the accepted norms (i.e., social norm compliance). To guarantee this, however, social norms need to be enforced by sanctioning those who violate them (i.e., social norm enforcement). Social norm compliance and enforcement are possible if at least the following conditions are met: the expectancy of behavior following shared norms, the ability to detect behaviors that deviate from those expected norms, and the selection of appropriate actions based on these deviations (Montague and Lohrenz, 2007).

Economic games —played as single or multiple iterations— are a powerful and reliable tool to investigate people's cognitive and affective processes toward social normative behavior. The *trust* (or *investment*) *game* (measuring the reciprocity norm) (TG; Berg et al., 1995; Camerer and Weigelt, 1988) and the *ultimatum game* (measuring the fairness norm) (UG; Güth et al., 1982) elicit in players social norms that trigger norm-compliant and norm-enforcing behaviors. Moreover, although measuring different social norms, both games have the same characteristics regarding the intentions and the outcomes, which play a crucial key role in the case of a social norm violation (Harth and Regner, 2016; McCabe et al., 2003; Xiang et al., 2013). In particular, involved players evaluate the intentions and value the outcomes before or after a social norm violation occurs.

In the TG, two players take the role of a *trustor* or a *trustee*. The trustor (i.e., investor) decides to pass any portion of an initial endowment to the trustee (i.e., an index of trusting behavior). This amount is usually tripled by the experimenter and the trustee decides to pass any portion back to the trustor (i.e., an index of reciprocity behavior) (Berg et al., 1995; Camerer, 2003a; Chaudhuri and Gangadharan, 2007; Csukás et al., 2008). During this sequential economic exchange, trustors usually invest more than half of their initial endowment and expect that the trustee will reciprocate their trust (Camerer, 2003b). However, when trustors know that their partners are likely to violate the norm of reciprocity and intend to betray their trust, investments are reduced by about one-third (Aimone and Houser, 2012; Aimone and Houser, 2013; Bohnet and Zeckhauser, 2004). Such expectations imply inferences of the intentions of the partner in the attempt to predict their behavior and previous evidence has shown that trustors' decisions are sensitive to other players' intentions (McCabe et al., 2003). For example, trustors send more money when reciprocity depends on a "partner" as opposed to an "opponent", suggesting that trustors only put trust in their partner when expectations of reciprocity are reasonable according to the partner's intentions (Burnham et al., 2000). In addition, previous or iterated experience with the same partner (like in the iterative TG) increases trusting behavior over time, because trust decisions can be based on feedback learning mechanisms about the partner's social behavior (Bellucci et al., 2017; Chang et al., 2010; Krueger et al., 2007). On the contrary, in single interactions (like in the one-shot TG), trustors have to assume that the partner would comply with the accepted social norms without any guarantee that she will, manifesting a strong betrayal aversion (Bohnet et al., 2008; Bohnet and Zeckhauser, 2004).

Similarly, trustees are also sensitive to the norm of reciprocity and return money to restore equality in payoff outcomes (Chang et al., 2011; McCabe et al., 2003). Having more money than their partner after being trusted induces aversive feelings (e.g., guilt), which makes a betrayal less appealing and motivates reciprocating behavior (Chang et al., 2011; Fehr and Schmidt, 1999; Rutledge et al., 2016). This suggests that norm-enforcing behavior during reciprocity builds on emotional processes related to unequal outcomes. Alike, when trustees do not feel compelled to enforce a reciprocity norm (for instance, when trustors threat to sanction defection), reciprocity rate drops notably, suggesting a cognitive shift from norm-sensitive to utility-based behavior (Fehr and Fischbacher, 2003; Johnson and Mislin, 2011; Li et al., 2009).

In the UG, two players are assigned the role of a *proposer* or a *responder*. The proposer provides an offer in the form of a split of an initial endowment to the responder. The responder then can either accept or reject the offer and in the latter case both players receive nothing. Being aware of the fairness norm, proposers usually share about 40% of their endowments and responders expect proposers to behave fairly and not to share less (Oosterbeek et al., 2004; Ruff et al., 2013). Responders reject unfair offers when their expectations of a norm-compliant behavior is intentionally violated (Civai et al., 2010; Civai et al., 2012; Corradi-Dell'Acqua et al., 2013; Güroğlu et al., 2011). This intentional norm violation (due to an unequal resource distribution) triggers aversive feelings (e.g., anger) in responders either measured through ratings or modeled computationally (Camerer, 2003a; Fehr and Schmidt, 1999; Güth et al., 1982; Pillutla and Murnighan, 1996). By rejecting the unfair offer, responders incur personal costs to enforce the fairness norm via a costly punishment decision (Fehr and Gachter, 2002; Pillutla and Murnighan, 1996). Ultimately, as an index of norm-enforcing behavior, costly punishment intends to re-establish equality in resource distributions (Güth et al., 2000; Güth et al., 1982; Nelson, 2002; Zamir, 2001).

Over the last decade, functional magnetic resonance imaging (fMRI) combined with economic games (i.e., TG, UG) has highlighted the role of the anterior insula (AI) in signaling social norm compliance and facilitating enforcement behaviors (Bellucci et al., 2017; Feng et al., 2015; Montague and Lohrenz, 2007; Sanfey et al., 2003). The insular cortex has been implicated in the integration of autonomic and visceral information into emotional, cognitive, and motivational functions (Namkung et al., 2017). The left and right AI take on similar functional roles in processing aversive feelings (e.g., pain, disgust and unfairness) in different fashions, with the left AI representing general, amodal features of aversive experiences, while the right AI showing segregated activity patterns specific for different modalities of aversive feelings (Corradi-Dell'Acqua et al., 2016). Recent coordinate-based meta-analyses of fMRI studies using the TG and the UG have demonstrated that the right AI is consistently activated during decisions to trust in the one-shot TG and to reciprocate in the iterative TG (see also Methods) (Bellucci et al., 2017) and during decisions to reject offers in the one-shot UG (Feng et al., 2015; Gabay et al., 2014). However, it remains unclear whether different AI subregions represent cognitive processes that generate expectancy for norm compliance and aversive feelings that generate motivation to norm enforcement. Previous parcellation studies indicate that the AI can be subdivided into a dorsal AI (dAI) region associated with a cognitive network and a ventral AI (vAI) region linked to a affective network (Chang et al., 2013; Kelly et al., 2012; Kurth et al., 2010), suggesting that different clusters within the AI may be engaged in different cognitive or emotional functions across economic games.

Here, we performed a coordinate-based meta-analysis —implementing the activation likelihood estimation (ALE) method (Eickhoff et al., 2009)— to investigate the consistent activation patterns of the right AI across two economic exchange games (TG, UG) measuring different social norm behaviors. While single fMRI studies have small sample sizes that undermine the statistical power and reliability of their isolated findings (Feredoes and Postle, 2007; Raemaekers et al., 2007), a coordinate-based meta-analysis increases the population sample for better generalization by integrating data across several studies (Eickhoff et al., 2006; Price et al., 2005; Wager et al., 2007). Further, we employed meta-analytic connectivity mapping (MACM) and resting-state functional connectivity (RSFC) to investigate task-based and task-free functional connectivity of the dAI and vAI. An increasing number of meta-analytic neuroimaging studies have combined task-based (MACM) and task-free (RSFC) connectivity analyses to reveal converging connectivity patterns of a brain region (Eickhoff et al., 2017; Goodkind et al., 2015; Hardwick et al., 2015; Krall et al., 2015; Wang et al., 2015). Importantly, different connectivity patterns as revealed by these analyses indicate the presence of different brain modules underlying distinct functional roles (Eickhoff et al., 2017). Based on this evidence, we hypothesized that the dAI —because of its connectivity with a cognitive network— is consistently activated during social interactions, in which cognitive processes elicited by inferences about the intentions of others lead to an expectancy of social norm compliance. Further, we predicated, that the vAI —because of its connectivity with an affective network— is consistently activated during social interactions, in which aversive feelings elicited by unequal outcome distributions lead to a motivation to social norm enforcement.

Materials and Methods

Meta-Analysis

Literature search and selection. Independent meta-analyses of neuroimaging studies on trust and reciprocity (using the TG) and on response to unfairness (using the UG) were conducted. We performed a systematic online database search on PubMed, ISI Web of Science, and Google Scholar by entering various combinations of relevant search items (up to the November 16, 2016). For the meta-analysis on trust and reciprocity, we used the following key words: 'trust', 'trust game', 'trust game', 'trustor', 'investor', 'trustee', 'trustworthiness', 'reciprocity', 'fMRI', 'magnetic resonance imaging', and 'neuroimaging'. For the meta-analysis on responses to fairness, we used 'normative decision making', 'fair', 'altruistic punishment', 'ultimatum game', 'fMRI', 'magnetic resonance imaging', and 'neuroimaging'. In addition, we explored several other sources, including (i) the BrainMap database (http://brainmap.org), (ii) work cited in review papers, and (iii) direct searches on the names of frequently occurring authors. The searched studies were further assessed according to the following criteria: (i) participants were free from psychiatric or neurological diagnoses; (ii) participants played different roles in the TG or UG; (iii) fMRI was used as the imaging modality; (iv) whole-brain general linear model analyses were applied (excluding region of interest [ROI] analyses); and (v) activations were presented in a standardized stereotaxic space (Talairach or Montreal Neurological Institute, MNI). Note that for studies reporting Talairach coordinates, a conversion to the MNI coordinates was implemented in the GingerALE software (https://www.brainmap.org/ale/) with the Brett's algorithm.

Activation Likelihood Estimation (ALE) approach. A coordinate-based meta-analysis was conducted, using the ALE algorithm (in-house MATLAB scripts) (Eickhoff et al., 2009). The ALE algorithm determines the convergence of foci reported from different functional (e.g., blood-oxygen-level dependent [BOLD] contrast imaging) or structural (e.g., voxel-based morphometry) neuroimaging studies with published foci in Talairach or MNI space (Laird et al., 2005a; Turkeltaub et al., 2002). It interprets reported foci as spatial probability distributions, whose widths are based on empirical estimates of the spatial uncertainty due to the between-subject and between-template variability of the neuroimaging data (Eickhoff et al., 2009). The ALE algorithm weights the between-subject variability based on the number of subjects analyzed in the studies, modeling larger sample sizes with smaller Gaussian distributions and thus presupposing more reliable approximation to the 'true' activation for larger sample sizes (Eickhoff et al., 2009).

The union of the individual modulated activation maps firstly created from the maximum probability associated with any one focus (always the closest one) for each voxel (Turkeltaub et al., 2012) is then calculated to obtain an ALE map across studies. This ALE map is assessed against a null-distribution of random spatial association between studies using a non-linear histogram integration algorithm (Eickhoff et al., 2012; Turkeltaub et al., 2012). The P value maps were thresholded using a cluster-level family-wise error (FWE) correction at $P < 0.05$ with a cluster defining threshold of $P < 0.001$ and 10,000 permutations (Eickhoff et al., 2012; Eklund et al., 2016). Moreover, given the low number of experiments in our meta-analysis (specially for decisions to trust in one-shot TG, see below), clusters were only considered as significant if: (i) their contributions were derived from at least two publications to avoid that only a single study may have driven the results and (ii) the most dominant experiment (MDE) contributed to the significant cluster on average less than 50% and the two MDEs (2MDEs) contributed on average less than 80% to meet criteria of robust, unbiased results as suggested by a recent simulation study (Eickhoff et al., 2016). To determine experiments' contributions, the fraction of the ALE value accounted for by each experiment contributing to the cluster was computed. This average non-linear contribution of each experiment to the ALE value was calculated from the ratio of the ALE values at the location of the cluster with and without the experiment in question (Eickhoff et al., 2016). Note that to localize the clusters within the AI the consistent activation maps were overlapped with the AI masks derived from Kurth et al. (2010) for all ALE meta-analyses.

First, ALE meta- analyses were performed across the different behaviors in each of the games. For the TG (**Tab. S1**), the ALE analyses included the following experiments (i.e., defined as a contrast within an fMRI study): (i) 13 experiments (52 peak foci across 130 subjects) for decisions to trust in the one-shot TG in which participants make a single (one-shot) trust decisions for each of their partners; (ii) 28 experiments (129 peak foci across 457 subjects) for decisions to trust in the iterative TG in which participants make iterative trust decisions for each of their partners; and (iii) 16 experiments (176 peak foci across 166 subjects) for decisions to reciprocate in the iterative TG in which participants make iterative reciprocity decisions for each of their partners. For the UG, the ALE meta-analyses included the following experiments: (iv) 27 experiments (309 peak foci across 871 subjects) for decisions to reject offers and (v) 15 experiments (61 peak foci across 464 subjects) for decisions to accept offers in the one-shot UG in which participants make a single (one-shot) decision for each of their partners (**Tab. S3**). Importantly, all games were multiplayer games in which participants made either one or iterative decisions with more than one partner. Next, conjunction analyses were performed to examine correspondence of these decisions across games. Finally, it has to be noted that we did not include contrasts for reciprocity decisions in the one-shot TG, distrust decisions in the iterative TG and decisions to propose offers in the one-shot UG, because we could not find enough published studies reporting contrasts for these decisions to reach a reasonable number of experiments and identify reliable results (Eickhoff et al., 2016).

Task-based connectivity: MACM analyses for dorsal and ventral AI

To further investigate commonalities and distinctions of the functional roles of the two AI regions, two independent MACM analyses were conducted with the dAI and vAI as seed regions (i.e., sphere ROIs of 10 mm around the peak coordinates of the previous conjunction analyses). MACM is a new approach to the analysis of functional connectivity, which delineates patterns of co-activation across thousands of studies using neuroimaging databases and produces data-driven functional connectivity maps based on pre-defined ROIs (Langner et al., 2014). MACM allows to probe co-activation patterns, i.e., task-based functional connectivity, across a wide range of behaviors and experimental settings. It has been shown that co-activation patterns revealed by MACM analyses share many features with resting-state functional connectivity patterns, but that both approaches also reveal idiosyncratic patterns related to the different metal states they are based on, i.e., task or rest (Jakobs et al., 2012; Reid et al., 2017). This duality is not surprising, as both methods are fundamentally aimed at revealing the same interaction patterns within large scale networks but do so under a different context and using a different set of data. The BrainMap database (http://www.brainmap.org/) was used, which at the time of assessment contained coordinates of reported activation foci and associated meta-data of approximately 8,400 neuroimaging experiments pertaining to "normal mapping" analyses (Laird et al., 2009). These reflect activations for whole brain neuroimaging contrasts in standard space for between-condition contrasts in healthy adult populations. Studies investigating between-group contrasts (e.g., related to age, gender or handedness), effects of intervention contrasts (e.g., pharmacological challenges, training), and clinical population contrasts were not considered. Importantly, MACM analyses cover experiments in the BrainMap database associated with different types of tasks that involve AI activations (Laird et al., 2005b). These analyses consisted of the following two steps. First, experiments in the BrainMap database were first identified that report at least one focus of activation within the dAI/vAI as ROIs. Second, ALE meta-analyses were conducted over all foci of the retrieved experiments to quantify their convergence and co-activation with each ROI (dAI, vAI). A total of 296 experimental contrasts and 5418 foci collected from 4,224 participants were identified for the dAI and 295 experimental contrasts and 4,891 foci collected from 4,362 participants for the vAI. The ALE maps were thresholded at $P < 0.05$ cluster-level corrected (cluster-forming threshold: $P < 0.001$ at voxel-level) and converted into Z-scores for display.

Task-free connectivity: RSFC analyses for dorsal and ventral AI

To complement task-based connectivity derived from MACM analyses, task-free connectivity was assessed with whole-brain RSFC analyses using dAI and vAI as seed regions (with each a sphere ROI of 10 mm). Two independent resting-state fMRI (rs-fMRI) datasets were collected on a 3 T and a 7 T scanner to identify the consistency of the resting-state networks under different signal-to-noise contributions for low-frequency BOLD fluctuations under rest: a 3 T dataset (89 participants: 45 male; 21.76±2.22 years old; range, 18-27; Beijing Normal University, China) and a 7 T dataset (77 participants: 33 males; 22.49±2.75 years old; range, 19-29; Auburn University, USA). During rs-fMRI scanning, participants were instructed to close their eyes, keep still, remain awake, and not think about anything systematically. Both studies were conducted in accordance with the Declaration of Helsinki and approved by the local Ethics Committee. Written informed consents were obtained from all participants, who were all right-handed and had no history of neurological or psychiatric disorders.

Image acquisition. The 3 T dataset was acquired with a Siemens TRIO 3 Tesla scanner at the Beijing Normal University Imaging Center for Brain Research. The rs-fMRI scan consisted of 150 contiguous volumes acquired with an echo-planar imaging (EPI) sequence (axial slices, 33; slice thickness, 3.5 mm; interslice gap, 0.7 mm; TR, 2000 ms; TE, 30 ms; flip angle, 90°; voxel size, 3.5×3.5×3.5 mm^3; FOV, 244×244 mm^2), whereas high-resolution structural images were acquired with a 3D sagittal T1-weighted magnetization-prepared rapid acquisition with gradient-echo (MP-RAGE) sequence (sagittal slices, 144; TR, 2530 ms; TE, 3.39 ms; slice thickness, 1.33 mm; voxel size, 1×1×1.33 mm^3; flip angle, 7°; inversion time, 1100ms; FOV, 256×256 mm^2). The 7 T dataset was collected with a Siemens MAGNETOM 7 Tesla scanner at the Auburn University MRI Research Center. The rs-fMRI scan consisted of 660 contiguous volumes acquired with an EPI sequence (axial slices, 45; slice thickness, 2.0 mm; interslice gap, 0.4 mm; slice acceleration factor, 3; TR, 1000 ms; TE, 20 ms; flip angle, 70°; voxel size, $2.1\times2.1\times2.0$ mm^3; FOV, 200×200 mm^2), whereas high-resolution structural images were acquired through a 3D sagittal T1-weighted MP-RAGE (sagittal slices, 240; TR, 2020 ms; TE, 2.7 ms; slice thickness, 1.2 mm; voxel size, $1.1\times1.1\times1.2$ mm^3; flip angle, 7°; inversion time, 1050 ms; FOV, 215×215 mm^2).

Image preprocessing. Neuroimaging data analyses were performed with SPM12 (http://www.fil.ion.ucl.ac.uk/spm/software/spm12/) and Artifact Detection Tools (ART, https://www.nitrc.org/projects/artifact_detect/). The 7 T EPI images were first bias-corrected to reduce field inhomogeneity. Then the same preprocessing pipeline was applied to both datasets. The functional images were corrected for slice timing and realigned for head movement correction to the mean image. To normalize functional images, participants' structural brain images were first segmented and then all functional images were co-registered to their own structural images. The parameters derived from segmentation were used to normalize each participant's functional images into MNI space (resampling voxel size was $2\times2\times2$ mm^3). Subsequently, the images were spatially smoothed using a Gaussian filter ($4\times4\times4$ mm^3 full width at half maximum, FWHM) to decrease spatial noise. Furthermore, ART was employed to detect and reject artifact in the time series of functional images. An artifact was detected if the (i) head displacement in x, y, or z direction was greater than 2 mm from the previous frame; (ii) rotational displacement was greater than 0.02 radians from the previous frame, or (iii) global mean intensity in the image was greater than 3 standard deviations from the mean image intensity for the entire resting scan. Those outliers were subsequently included as nuisance regressors within the first-level general linear model. Finally, a band-pass filter (0.01~0.1 Hz) was implemented to remove high-frequency noise and linear drift artifacts.

Seed-to-Voxel connectivity. Implementing a seed-based analysis, the functional connectivity (bivariate correction) between the average BOLD signals from given seed regions (dAI and vAI) and all other voxels in the brain was computed using the Functional Connectivity (CONN) toolbox (https://www.nitrc.org/projects/conn). To remove potential sources of confounds, regressors of no interest were added in the first-level general linear model, including 6 head motion parameters (3 translations and 3 rotations along x, y, and z axes), outliers derived from the ART toolbox, white matter and cerebrospinal fluid signal. The Pearson's correlation coefficients obtained at each voxel were transformed into Fisher's *z* values to indicate the degree of connectivity between each ROI and the voxel.

First-level, subject-specific, connectivity maps for each ROI were then employed in a second-level analysis in which a paired t-test was performed to compare connectivity strength with dAI and vAI at each voxel. The calculated *t* images were subsequently thresholded at $P < 0.05$ cluster-level corrected (cluster-forming threshold: $P < 0.001$ at voxel-level). Finally, anatomical allocation for all significant coordinates was assessed using the SPM xjview toolbox (http://www.alivelearn.net/xjview/) and the automated anatomic labeling (AAL) atlas (Tzourio-Mazoyer et al., 2002).

Results

ALE Meta-Analyses

ALE meta-analyses revealed consistent activations in the right AI for decisions to (i) trust in one-shot TG (5 contributing contrasts; i.e., 38.5% of the total experiments, MDE=26.3%, 2MDEs=48.5%) (**Tab. 1 & Fig, 1a & Tab. S4**); (ii) reciprocate in iterative TG (10 contributing contrasts; i.e., 62.5% of the total experiments, MDE=18.5%, 2MDEs=34.6%) (**Tab. 1 & Fig. 1b & Tab. S4**); and (iii) reject unfair offers in one-shot UG (19 contributing contrasts; i.e., 70.4% of the total experiments: MDE=12.3%, 2MDEs=24.1%) (**Tab. 1 & Fig. 1c & Tab. S5**). No AI activations were found for decisions to accept fair offers or for trust decisions in the iterative TG.

Insert Figure 1 & Table 1 about here

Furthermore, consistent activation maxima for decisions to trust in iterative TG were found in the left ventral striatum (nucleus accumbens; 7 contributing contrasts, i.e., 25% of the total experiments: MDE=28.3%, 2MDEs=56.1%) (**Tab. 1 & Tab. S4**). Further, consistent activation maxima for decisions to reciprocate in in iterative TG were found in the right inferior parietal lobule (IPL, 6 contributing contrasts, i.e., 37.5% of the total experiments: MDE=21.6%, 2MDEs=41.4%); right inferior temporal gyrus (6 contributing contrasts, i.e., 37.5% of the total experiments: MDE=24.9%, 2MDEs=42.4%); and inferior occipital gyrus (5 contributing contrasts, i.e., 31.3% of the total experiments: MDE = 26.9%, 2MDEs = 52.8%) (**Tab. S4**). In addition, rejection of unfair offers in one-shot UG consistently activated the left AI (20 experimental contrasts, i.e., 74.1% of the total experiments: MDE=9.6%, 2MDEs=17.1%); anterior middle cingulate cortex (aMCC, 21 experimental contrasts, i.e., 77.8% of the total experiments: MDE=12.4%, 2MDEs=22.2%); and middle frontal gyrus in the dorsolateral prefrontal cortex (DLPFC, 2 clusters with 7 and 8 contributing contrasts, respectively, i.e., 25.9 and 29.6% of the total experiments: MDE=23.7 and 25.5%, 2MDEs=47.2 and 50.6%) (**Tab. S5**).

ALE Conjunction Analyses

After overlapping the identified AI clusters with the AI masks derived from Kurth et al. (2010), our conjunction analysis revealed a common activation maximum in the dAI during decisions to trust (one-shot TG) and to reject unfair offers (one-shot UG), (**Fig. 2a**) as well as a common activation maximum in the right vAI for decisions to reciprocate and decisions to reject unfair offers (**Fig. 2b**).

Insert Figure 2 about here

MACM and RSFC Analyses

Using ROIs around the peak coordinates of dAI and vAI identified in the previous conjunction analyses, task-based (MACM) and task-free (RSFC) connectivity analyses were conducted to further investigate the functional roles and connectivity patterns of dAI and vAI. MACM and RSFC analyses of both 3 T and 7 T datasets showed similar connectivity results. For the dAI, MACM analyses revealed functional connectivity with the middle frontal gyrus (DLPFC), aMCC, and inferior/superior parietal lobule (IPL/SPL) (**Tab. 2 & Fig. 3a**). For the vAI, they revealed functional connectivity patterns with limbic and somatosensory regions, including caudate/thalamus, brainstem, left precentral gyrus and SMA (**Tab. 2 & Fig. 3b**).

Insert Figure 3 & Table 2 about here

RSFC analyses revealed that task-free functional connectivity patterns for both datasets (3 T & 7 T) were closely overlapping with each other. In particular, the dAI compared to vAI was more strongly functionally connected with prefrontal (DLPFC) and parietal regions (IPL) (**Tab. 3 & Fig. 3c**), while the vAI compared to the dAI was more strongly connected with the orbitofrontal cortex, ventral anterior cingulate cortex (ACC), angular gyrus, and temporal lobe (**Tab. 3 & Fig. 3d**). In addition to the MACM results, RSFC analyses revealed a clearer distinctive functional connectivity patterns of these two insular regions with the vAI predominantly connected with medial prefrontal regions (medial prefrontal cortex, ventral ACC) and the dAI connected with more posterior (MCC and SMA) and lateral frontoparietal regions (DLPC and IPL) (**Fig. 3**).

Insert Table 3 about here

Conjunction analyses between MACM and RSFC results (on both datasets) showed that the dAI was significantly connected with regions of a cognitive control network, such as DLPFC, IPL and aMCC/supplementary motor area (SMA) (**Tab. 4 & Fig. 4a**), while the vAI was significantly connected with regions associated with the sensory and emotional domain such as the ACC, SMA and caudate (**Tab. 4 & Fig. 4b**).

Insert Figure 4 & Table 4 about here

Discussion

We combined coordinate-based fMRI meta-analyses with task-based and task-free connectivity analyses to study the role of the AI in social norm compliance and social norm enforcement in two economic games (TG, UG). Our meta-analysis findings showed that the right AI was the only common brain region consistently activated across both games. Further, our results demonstrated a variable clustering depending on the role assumed in these games with a cluster in the right dAI for decisions to trust and to reject unfair offers, and a cluster in the vAI for decisions to reciprocate and to reject unfair offers. Our task-based and task-free connectivity analyses showed that these two clusters were part of two functionally distinguishable connectivity networks mostly associated with cognitive (dAI) and emotional (vAI) processes, a similar distinction that has been previously shown for the anterior cingulate cortex (e.g., Behrens et al., 2008). We argue that in circumstances of a social norm violation (hypothetical or actual), the dAI mediates cognitive processes associated with an expectancy of social norm compliance, whereas vAI mediates affective processes associated with inequality aversion that lead to social norm enforcement.

First, expectancy of social norm compliance requires the representation of the norms, the ability to detect deviations from the expected norm behaviors, and the selection of appropriate actions based on these deviations (Montague and Lohrenz, 2007). Both the trustor in the one-shot TG and the responder to unfair offers in the one-shot UG may engage in these cognitive processes to predict (in the case of trustors) or to comprehend (in the case of responders) their partner's behavior. The resulting expectations underlie a decision to trust or to reject unfair offers, which consistently activated the dAI. This AI region has previously been shown to be part of a cognitive network associated with higher-order cognition (Chang et al., 2013; Deen et al., 2011; Kurth et al., 2010). As opposed to the vAI, our connectivity analyses provided some evidence to a distinctive connectivity pattern of the dAI, which was mostly associated with frontoparietal, cortical regions.

Within the cognitive domain, the dAI has been associated with language (Mutschler et al., 2009), working memory (Mayer et al., 2007), and attention (Nelson et al., 2010), and in social contexts with anticipation of negative and unknown events (Baumgartner et al., 2009; Herwig et al., 2007a; Herwig et al., 2007b), threat of punishment (Spitzer et al., 2007), and fairness-norm violation (Sanfey et al., 2003). Since the dAI is responsive to different types of violations (Dosenbach et al., 2006), including violation of musical (Koelsch et al., 2002), tactile (Allen et al., 2016) and visuo-motor (Farrer and Frith, 2002) expectancies, we argue that this region mediates cognitive processes signaling an intentional norm violation.

On the one hand, we suggest that dAI activity in trustors playing a one-shot TG likely underlies inferences on a *hypothetical norm violation* by the trustee. As the trustor has no information about the partner's social behavior, their decision is entirely based on the expectation that the trustee complies with the norm to reciprocate trust (Aimone and Houser, 2012; Aimone and Houser, 2013; Bohnet and Zeckhauser, 2004). Therefore, an absence of concerns for an intentional norm violation should lead to more trusting behavior and a decrease in dAI activity. Indeed, trustors have been observed to send more money and engage the right dAI less when interacting with a computer mediator compared to a human player (Aimone et al., 2014). Similarly, when a cooperative relationship of trust and reciprocity is established over the course of multiple interactions like in an iterative TG, trustors do not expect any intentional norm violation. Instead, they know that the partner will most probably cooperate and can thus predict the positive outcome after a decision to trust, which consistently activated the ventral striatum in our previous meta-analysis (see also, Bellucci et al., 2017).

On the other hand, we suggest that the dAI in responders rejecting unfair offers during one-shot UGs might mediate inferences on an *actual norm violation* by the proposer. Responders in UGs expect that proposers comply with a fairness norm splitting their initial endowment equally (Guo et al., 2014; Guo et al., 2013; Sanfey, 2007; Sanfey et al., 2003). When receiving an unfair offer, they face an intentional violation of the norm of fairness that took already place and makes them reject the offer. On the contrary, receiving a fair offer should increase acceptance behavior and decrease dAI activity. The same results should be observed also when the unfairness of a split is not to trace back to an intentional norm violation by the partner. In line with this, the current meta-analysis found no right dAI activations in responders to fair offers whose expectations are arguably not violated but rather fulfilled by their proposers. Further, a previous study has shown lower rejection rates and lower activity in the right dAI in response to unintentional unfair offers, namely when proposers had no other alternative but offering an unfair split, but higher dAI activity for acceptance of intentional unfair offers (Güroğlu et al., 2011).

Second, after detecting deviations from the expected norm behaviors, social norms get enforced when social concerns are strong enough to motivate people to enact on their knowledge about socially accepted behavior (Blake and McAuliffe, 2011). Aversive feelings toward social injustices appear to play an important motivational role in social norm enforcement (Harle et al., 2012; Osumi and Ohira, 2010; Pillutla and Murnighan, 1996). Both the trustee reciprocating in iterative TGs and the responder rejecting unfair offers in one-shot UGs face unequal resource distributions, being either in an advantageous or disadvantageous situation, respectively. Aversive feelings toward this inequality induce reciprocating and rejecting behaviors, which consistently activated the vAI. The vAI has previously been demonstrated to be part of a network associated with emotional processing (Deen et al., 2011; Kurth et al., 2010). <u>Our connectivity analyses suggest that the vAI is mostly connected to subcortical and medial cortical brain regions, indicating a distinctive connectivity pattern of the vAI as opposed to the dAI.</u> This region is not only involved in emotional processing, including anger (Krämer et al., 2007), disgust (Calder et al., 2007; Wicker et al., 2003) and pain (Singer et al., 2004), but also in processes related to socially-relevant emotions, including social pain

(Meyer et al., 2015), social exclusion (Eisenberger et al., 2003), and empathy (Klimecki et al., 2014; Singer et al., 2004). Since the vAI signals aversive feelings elicited by different forms of injustice within the social domain (Decety and Yoder, 2016; Harle et al., 2012), we argue that this region likely mediates inequality aversions that motivate norm enforcement.

On the one hand, we suggest that the vAI probably signals an *advantageous inequality aversion* in trustees during iterative TGs. As trustees usually end up having more than their partner, they may anticipate feelings of guilt when considering betraying their partner and defecting, which implies a potential violation of the norm of reciprocity (Charness and Dufwenberg, 2006; Krajbich et al., 2009). Trustees' sensitivity toward inequality aversion may thus make them feel compelled to reciprocate trust through cooperation (Eriksson and Simpson, 2011; Fehr and Schmidt, 1999), especially in iterated and non-anonymous interactions in which concerns for social status and reputation play a pivotal role (McAuliffe et al., 2013; Milinski et al., 2002; Nowak and Sigmund, 1998). In contrast, we would expect looser sensitivity to advantageous inequality and no vAI activation in circumstances in which self-interested behaviors are less detrimental, such as in single and anonymous interactions (Ariely et al., 2009; Johnson and Mislin, 2011; Semmann et al., 2004). Previous studies have shown that advantageous offers are rejected less in an anonymous UG (Civai et al., 2012) and no vAI activations were observed during decisions to reciprocate in one-shot TGs (Nihonsugi et al., 2015; van den Bos et al., 2009, 2011). Thus, like for empathy (Singer et al., 2006; Zheng et al., 2016), reputation may modulate vAI responses to advantageous inequality as well, and motivate people to refrain from intentionally violating a social norm.

On the other hand, we suggest that the vAI may signal a *disadvantageous inequality aversion* in responders rejecting unfair offers in one-shot UGs. Aversive feelings such as anger are arguably elicited in responders to unfair offers (Fehr and Schmidt, 1999; Pillutla and Murnighan, 1996), who need to deal with an intentional violation of a fairness norm when receiving an unequal split. Previous studies have shown that inequality aversion motivates responders to unfair offers to enforce the norm of fairness via the costly punishment of a rejection (Yu et al., 2014). This concurs with previous evidence indicating that the absence of emotional responses to unfair offers is associated with higher acceptance rates and reduced norm-enforcing behavior (Osumi and Ohira, 2010). Our results further revealed that responders to fair offers, who do not suffer a distributive injustice from their proposers, do not to engage the vAI. In accordance with our findings, vAI activity has been particularly observed when facing disadvantageous inequality, and decreases for increasingly accepted unfair offers, suggesting a link between vAI activation and norm enforcement (Tabibnia et al., 2008; Yu et al., 2014).

Taken together, the insula cortex is an underestimated brain region whose importance has been rediscovered not only in the understanding of human cognition but also in neurological disorders (Namkung et al., 2017). Previous work has already begun to characterize anatomical and functional differentiations of the insular cortex. Using a coordinate-based meta-analysis approach, we showed consistent differential AI activation patterns across economic games measuring social norms of reciprocity (TG) and fairness (UG). Confirmed by our task-based and task-free connectivity analyses, the dAI and vAI revealed diverse functional connectivity patterns indicating their different roles in the context of hypothetical or real violations of social norms. In particular, the dAI likely mediates cognitive processes associated with expectancy of social norm compliance, whereas the vAI arguably mediates inequality aversion linked to social norm enforcement.

Although this is the first study to reveal different functionality of subregions of the AI within the social domain, our study has a couple of limitations that need to be addressed in future investigations. First, due to a lack of fMRI studies, decisions to reciprocate in the one-shot TG, decisions to distrust in the iterative TG and decisions to propose offers in the one-shot UG could not be analyzed in the current coordinate-based meta-analysis. To confirm our assumptions about the role of AI subregions, future neuroimaging studies are needed to investigate decisions in the TG and UG across all player positions (first or second decision-maker) and game iteration types (one-shot, iterative) as well as different decisions in the same game (e.g., trusting and distrusting in a iterative TG) or decisions in additional economic games (e.g., prisoner's dilemma game, communication game) measuring different normative behaviors. Second, since our meta-analytic findings are based on the consistent activations found in previous fMRI studies, future investigations employing targeted experimental manipulations are needed to confirm our interpretations of the different functions of these AI subregions.

Despite these limitations, our study is one of the few investigations mapping the topographic organization of a brain region with across-tasks and across-modalities analyses for a better characterization of its functional role (Eickhoff et al., 2017). Moreover, our results provide a distinctive mapping of the dAI and vAI with standardized coordinates that can be used in future studies to test further hypotheses on the functioning of the AI in social cognition (e.g., whether its activation patterns reflect interindividual differences in social behaviors), thereby contributing to a more comprehensive understanding of this region for both basic and clinical neuroscience.

Acknowledgments:

This work was supported by the German Federal Ministry of Education and Research (P-57191936 to F. K.), the National Institute of Mental Health (R01-MH074457), the Helmholtz Portfolio Theme "Supercomputing and Modelling for the Human Brain", the European Union Seventh Framework Program (FP7/2007-2013) under grant agreement no. 7202070 (to S. B. E.), the National Postdoctoral Program for Innovative Talents under grant agreement no. BX201600019 (to C. F.), and the China Postdoctoral Science Foundation under grant agreement no. 2017M610055 (to C.F.).

Conflict of Interest

The authors are unaware of any conflicts of interest, financial or otherwise.

References

Aimone, J.A., Houser, D., 2012. What you don't know won't hurt you: a laboratory analysis of betrayal aversion. Experimental Economics 15, 571-588.

Aimone, J.A., Houser, D., 2013. Harnessing the benefits of betrayal aversion. Journal of Economic Behavior & Organization 89, 1-8.

Aimone, J.A., Houser, D., Weber, B., 2014. Neural signatures of betrayal aversion: an fMRI study of trust. Proceedings of the Royal Society B: Biological Sciences 281, 20132127.

Allen, M., Fardo, F., Dietz, M.J., Hillebrandt, H., Friston, K.J., Rees, G., Roepstorff, A., 2016. Anterior insula coordinates hierarchical processing of tactile mismatch responses. Neuroimage 127, 34-43.

Ariely, D., Bracha, A., Meier, S., 2009. Doing Good or Doing Well? Image Motivation and Monetary Incentives in Behaving Prosocially. American Economic Review 99, 544-555.

Baumgartner, T., Fischbacher, U., Feierabend, A., Lutz, K., Fehr, E., 2009. The neural circuitry of a broken promise. Neuron 64, 756-770.

Behrens, T.E., Hunt, L.T., Woolrich, M.W., Rushworth, M.F., 2008. Associative learning of social value. Nature 456, 245-249.

Bellucci, G., Chernyak, S.V., Goodyear, K., Eickhoff, S.B., Krueger, F., 2017. Neural signatures of trust in reciprocity: A coordinate-based meta-analysis. Hum Brain Mapp 38, 1233-1248.

Berg, J., Dickhaut, J., McCabe, K., 1995. Trust, Reciprocity &Social History. Games and Economic Behavior 10, 122-142.

Bicchieri, C., 1990. Norms of Cooperation. Ethics 100, 838-861.

Bicchieri, C., 2005. The Grammar of Society: The Nature and Dynamics of Social Norms. Cambridge University Press, Cambridge.

Bicchieri, C., 2014. Norms, conventions, and the power of expectations, in: Cartwright, N., Montuschi, E. (Eds.), Philosophy of social science: A new introduction. Oxford University Press, Oxford, pp. 208-229.

Blake, P.R., McAuliffe, K., 2011. "I had so much it didn't seem fair": Eight-year-olds reject two forms of inequity. Cognition 120, 215-224.

Bohnet, I., Greig, F., Herrmann, B., Zeckhauser, R., 2008. Betrayal Aversion: Evidence from Brazil, China, Oman, Switzerland, Turkey, and the United States. American Economic Review 98, 294-310.

Bohnet, I., Zeckhauser, R., 2004. Trust, risk and betrayal. Journal of Economic Behavior & Organization 55, 467-484.

Buckholtz, J.W., Marois, R., 2012. The roots of modern justice: cognitive and neural foundations of social norms and their enforcement. Nat Neurosci 15, 655-661.

Burnham, T., McCabe, K., Smith, V.L., 2000. Friend-or-foe intentionality priming in an extensive form trust game. Journal of Economic Behavior & Organization 43, 57-73.

Calder, A.J., Beaver, J.D., Davis, M.H., van Ditzhuijzen, J., Keane, J., Lawrence, A.D., 2007. Disgust sensitivity predicts the insula and pallidal response to pictures of disgusting foods. Eur J Neurosci 25, 3422-3428.

Camerer, C., Weigelt, K., 1988. Experimental Tests of a Sequential Equilibrium Reputation Model. Econometrica 56, 1-36.

Camerer, C.F., 2003a. Behavioral game theory : experiments in strategic interaction. Russell Sage Foundation; Princeton University Press, New York, N.Y., Princeton, N.J.

Camerer, C.F., 2003b. Behavioural studies of strategic thinking in games. Trends in Cognitive Sciences 7, 225-231.

Chang, L.J., Doll, B.B., van 't Wout, M., Frank, M.J., Sanfey, A.G., 2010. Seeing is believing: trustworthiness as a dynamic belief. Cogn Psychol 61, 87-105.

Chang, L.J., Smith, A., Dufwenberg, M., Sanfey, A.G., 2011. Triangulating the neural, psychological, and economic bases of guilt aversion. Neuron 70, 560-572.

Chang, L.J., Yarkoni, T., Khaw, M.W., Sanfey, A.G., 2013. Decoding the role of the insula in human cognition: functional parcellation and large-scale reverse inference. Cereb Cortex 23, 739-749.

Charness, G., Dufwenberg, M., 2006. Promises and Partnership. Econometrica 74, 1579-1601.

Chaudhuri, A., Gangadharan, L., 2007. An experimental analysis of trust and trustworthiness. Southern

Economic Journal 73, 959-985.
Civai, C., Corradi-Dell'Acqua, C., Gamer, M., Rumiati, R.I., 2010. Are irrational reactions to unfairness truly emotionally-driven? Dissociated behavioural and emotional responses in the Ultimatum Game task. Cognition 114, 89-95.
Civai, C., Crescentini, C., Rustichini, A., Rumiati, R.I., 2012. Equality versus self-interest in the brain: differential roles of anterior insula and medial prefrontal cortex. Neuroimage 62, 102-112.
Corradi-Dell'Acqua, C., Civai, C., Rumiati, R.I., Fink, G.R., 2013. Disentangling self- and fairness-related neural mechanisms involved in the ultimatum game: an fMRI study. Social cognitive and affective neuroscience 8, 424-431.
Corradi-Dell'Acqua, C., Tusche, A., Vuilleumier, P., Singer, T., 2016. Cross-modal representations of first-hand and vicarious pain, disgust and fairness in insular and cingulate cortex. Nat Commun 7, 10904.
Csukás, C., Fracalanza, P., Kovács, T., Willinger, M., 2008. The determinants of trusting and reciprocal behaviour: evidence from an intercultural experiment. Journal of Economic Development 33, 71-95.
Decety, J., Yoder, K.J., 2016. The Emerging Social Neuroscience of Justice Motivation. Trends in Cognitive Sciences.
Deen, B., Pitskel, N.B., Pelphrey, K.A., 2011. Three systems of insular functional connectivity identified with cluster analysis. Cereb Cortex 21, 1498-1506.
Dosenbach, N.U., Visscher, K.M., Palmer, E.D., Miezin, F.M., Wenger, K.K., Kang, H.C., Burgund, E.D., Grimes, A.L., Schlaggar, B.L., Petersen, S.E., 2006. A core system for the implementation of task sets. Neuron 50, 799-812.
Eickhoff, S.B., Amunts, K., Mohlberg, H., Zilles, K., 2006. The human parietal operculum. II. Stereotaxic maps and correlation with functional imaging results. Cerebral cortex 16, 268-279.
Eickhoff, S.B., Bzdok, D., Laird, A.R., Kurth, F., Fox, P.T., 2012. Activation likelihood estimation meta-analysis revisited. Neuroimage 59, 2349-2361.
Eickhoff, S.B., Constable, R.T., Yeo, B.T., 2017. Topographic organization of the cerebral cortex and brain cartography. Neuroimage.
Eickhoff, S.B., Laird, A.R., Grefkes, C., Wang, L.E., Zilles, K., Fox, P.T., 2009. Coordinate-based activation likelihood estimation meta-analysis of neuroimaging data: A random-effects approach based on empirical estimates of spatial uncertainty. Human brain mapping 30, 2907-2926.
Eickhoff, S.B., Nichols, T.E., Laird, A.R., Hoffstaedter, F., Amunts, K., Fox, P.T., Bzdok, D., Eickhoff, C.R., 2016. Behavior, sensitivity, and power of activation likelihood estimation characterized by massive empirical simulation. Neuroimage 137, 70-85.
Eisenberger, N.I., Lieberman, M.D., Williams, K.D., 2003. Does rejection hurt? An FMRI study of social exclusion. Science 302, 290-292.
Eklund, A., Nichols, T.E., Knutsson, H., 2016. Cluster failure: Why fMRI inferences for spatial extent have inflated false-positive rates. Proceedings of the National Academy of Sciences of the United States of America 113, 7900-7905.
Eriksson, K., Simpson, B., 2011. Perceptions of unfairness in allocations between multiple recipients. Cogn Psychol 62, 225-244.
Farrer, C., Frith, C.D., 2002. Experiencing oneself vs another person as being the cause of an action: the neural correlates of the experience of agency. Neuroimage 15, 596-603.
Fehr, E., Fischbacher, U., 2003. The nature of human altruism. Nature 425, 785-791.
Fehr, E., Gachter, S., 2002. Altruistic punishment in humans. Nature 415, 137-140.
Fehr, E., Schmidt, K.M., 1999. A theory of fairness, competition, and cooperation. Quarterly Journal of Economics 114, 817-868.
Feng, C., Luo, Y.-J., Krueger, F., 2015. Neural signatures of fairness-related normative decision making in the ultimatum game: A coordinate-based meta-analysis. Human Brain Mapping 36, 591-602.
Feredoes, E., Postle, B.R., 2007. Localization of load sensitivity of working memory storage: quantitatively and qualitatively discrepant results yielded by single-subject and group-averaged approaches to fMRI group analysis. Neuroimage 35, 881-903.
Gabay, A.S., Radua, J., Kempton, M.J., Mehta, M.A., 2014. The Ultimatum Game and the brain: a meta-analysis of neuroimaging studies. Neurosci Biobehav Rev 47, 549-558.

Goodkind, M., Eickhoff, S.B., Oathes, D.J., Jiang, Y., Chang, A., Jones-Hagata, L.B., Ortega, B.N., Zaiko, Y.V., Roach, E.L., Korgaonkar, M.S., Grieve, S.M., Galatzer-Levy, I., Fox, P.T., Etkin, A., 2015. Identification of a common neurobiological substrate for mental illness. JAMA Psychiatry 72, 305-315.

Guo, X., Zheng, L., Cheng, X., Chen, M., Zhu, L., Li, J., Chen, L., Yang, Z., 2014. Neural responses to unfairness and fairness depend on self-contribution to the income. Social cognitive and affective neuroscience 9, 1498-1505.

Guo, X., Zheng, L., Zhu, L., Li, J., Wang, Q., Dienes, Z., Yang, Z., 2013. Increased neural responses to unfairness in a loss context. Neuroimage 77, 246-253.

Güroğlu, B., van den Bos, W., van Dijk, E., Rombouts, S.A., Crone, E.A., 2011. Dissociable brain networks involved in development of fairness considerations: understanding intentionality behind unfairness. Neuroimage 57, 634-641.

Güth, W., Königstein, M., Marchand, N., Nehring, K., 2000. Trust and Reciprocity in the Investment Game with Indirect Reward. Homo Oeconomicus XVIII, 241-262.

Güth, W., Schmittberger, R., Schwarze, B., 1982. An experimental analysis of ultimatum bargaining. Journal of Economic Behavior & Organization 3, 367-388.

Hardwick, R.M., Lesage, E., Eickhoff, C.R., Clos, M., Fox, P., Eickhoff, S.B., 2015. Multimodal connectivity of motor learning-related dorsal premotor cortex. Neuroimage 123, 114-128.

Harle, K.M., Chang, L.J., van 't Wout, M., Sanfey, A.G., 2012. The neural mechanisms of affect infusion in social economic decision-making: a mediating role of the anterior insula. Neuroimage 61, 32-40.

Harth, N.S., Regner, T., 2016. The spiral of distrust: (Non-)cooperation in a repeated trust game is predicted by anger and individual differences in negative reciprocity orientation. Int J Psychol.

Herwig, U., Baumgartner, T., Kaffenberger, T., Bruhl, A., Kottlow, M., Schreiter-Gasser, U., Abler, B., Jancke, L., Rufer, M., 2007a. Modulation of anticipatory emotion and perception processing by cognitive control. Neuroimage 37, 652-662.

Herwig, U., Kaffenberger, T., Baumgartner, T., Jancke, L., 2007b. Neural correlates of a 'pessimistic' attitude when anticipating events of unknown emotional valence. Neuroimage 34, 848-858.

Jakobs, O., Langner, R., Caspers, S., Roski, C., Cieslik, E.C., Zilles, K., Laird, A.R., Fox, P.T., Eickhoff, S.B., 2012. Across-study and within-subject functional connectivity of a right temporo-parietal junction subregion involved in stimulus-context integration. Neuroimage 60, 2389-2398.

Johnson, N.D., Mislin, A.A., 2011. Trust games: A meta-analysis. Journal of Economic Psychology 32, 865-889.

Kelly, C., Toro, R., Di Martino, A., Cox, C.L., Bellec, P., Castellanos, F.X., Milham, M.P., 2012. A convergent functional architecture of the insula emerges across imaging modalities. Neuroimage 61, 1129-1142.

Klimecki, O.M., Leiberg, S., Ricard, M., Singer, T., 2014. Differential pattern of functional brain plasticity after compassion and empathy training. Social cognitive and affective neuroscience 9, 873-879.

Koelsch, S., Gunter, T.C., v. Cramon, D.Y., Zysset, S., Lohmann, G., Friederici, A.D., 2002. Bach Speaks: A Cortical “Language-Network” Serves the Processing of Music. NeuroImage 17, 956-966.

Krajbich, I., Adolphs, R., Tranel, D., Denburg, N.L., Camerer, C.F., 2009. Economic games quantify diminished sense of guilt in patients with damage to the prefrontal cortex. J Neurosci 29, 2188-2192.

Krall, S.C., Rottschy, C., Oberwelland, E., Bzdok, D., Fox, P.T., Eickhoff, S.B., Fink, G.R., Konrad, K., 2015. The role of the right temporoparietal junction in attention and social interaction as revealed by ALE meta-analysis. Brain Struct Funct 220, 587-604.

Krämer, U.M., Jansma, H., Tempelmann, C., Münte, T.F., 2007. Tit-for-tat: the neural basis of reactive aggression. Neuroimage 38, 203-211.

Krueger, F., McCabe, K., Moll, J., Kriegeskorte, N., Zahn, R., Strenziok, M., Heinecke, A., Grafman, J., 2007. Neural correlates of trust. Proceedings of the National Academy of Sciences of the United States of America 104, 20084-20089.

Kurth, F., Zilles, K., Fox, P.T., Laird, A.R., Eickhoff, S.B., 2010. A link between the systems: functional differentiation and integration within the human insula revealed by meta-analysis. Brain Struct Funct 214, 519-534.

Laird, A.R., Eickhoff, S.B., Kurth, F., Fox, P.M., Uecker, A.M., Turner, J.A., Robinson, J.L., Lancaster, J.L., Fox, P.T., 2009. ALE meta-analysis workflows via the brainmap database: progress towards a

probabilistic functional brain atlas. Frontiers in neuroinformatics 3, 23.
Laird, A.R., Fox, P.M., Price, C.J., Glahn, D.C., Uecker, A.M., Lancaster, J.L., Turkeltaub, P.E., Kochunov, P., Fox, P.T., 2005a. ALE meta-analysis: Controlling the false discovery rate and performing statistical contrasts. Human brain mapping 25, 155-164.
Laird, A.R., Lancaster, J.L., Fox, P.T., 2005b. BrainMap: The Social Evolution of a Human Brain Mapping Database. Neuroinformatics 3, 065-078.
Langner, R., Rottschy, C., Laird, A.R., Fox, P.T., Eickhoff, S.B., 2014. Meta-analytic connectivity modeling revisited: controlling for activation base rates. NeuroImage 99, 559-570.
Li, J., Xiao, E., Houser, D., Montague, P.R., 2009. Neural responses to sanction threats in two-party economic exchange. Proceedings of the National Academy of Sciences of the United States of America 106, 16835-16840.
Mayer, J.S., Bittner, R.A., Nikolic, D., Bledowski, C., Goebel, R., Linden, D.E., 2007. Common neural substrates for visual working memory and attention. Neuroimage 36, 441-453.
McAuliffe, K., Blake, P.R., Kim, G., Wrangham, R.W., Warneken, F., 2013. Social influences on inequity aversion in children. PLoS One 8, e80966.
McCabe, K.A., Rigdon, M.L., Smith, V.L., 2003. Positive reciprocity and intentions in trust games. Journal of Economic Behavior & Organization 52, 267-275.
Meyer, M.L., Williams, K.D., Eisenberger, N.I., 2015. Why Social Pain Can Live on: Different Neural Mechanisms Are Associated with Reliving Social and Physical Pain. PLoS One 10, e0128294.
Milinski, M., Semmann, D., Krambeck, H.J., 2002. Reputation helps solve the 'tragedy of the commons'. Nature 415, 424-426.
Montague, P.R., Lohrenz, T., 2007. To detect and correct: norm violations and their enforcement. Neuron 56, 14-18.
Mutschler, I., Wieckhorst, B., Kowalevski, S., Derix, J., Wentlandt, J., Schulze-Bonhage, A., Ball, T., 2009. Functional organization of the human anterior insular cortex. Neurosci Lett 457, 66-70.
Namkung, H., Kim, S.H., Sawa, A., 2017. The Insula: An Underestimated Brain Area in Clinical Neuroscience, Psychiatry, and Neurology. Trends Neurosci.
Nelson, S.M., Dosenbach, N.U., Cohen, A.L., Wheeler, M.E., Schlaggar, B.L., Petersen, S.E., 2010. Role of the anterior insula in task-level control and focal attention. Brain Struct Funct 214, 669-680.
Nelson, W.R., 2002. Equity or intention: it is the thought that counts. Journal of Economic Behavior & Organization 48, 423-430.
Nihonsugi, T., Ihara, A., Haruno, M., 2015. Selective increase of intention-based economic decisions by noninvasive brain stimulation to the dorsolateral prefrontal cortex. J Neurosci 35, 3412-3419.
Nowak, M.A., Sigmund, K., 1998. Evolution of indirect reciprocity by image scoring. Nature 393, 573-577.
Oosterbeek, H., Sloof, R., van de Kuilen, G., 2004. Cultural Differences in Ultimatum Game Experiments: Evidence from a Meta-Analysis. Experimental Economics 7, 171-188.
Osumi, T., Ohira, H., 2010. The positive side of psychopathy: Emotional detachment in psychopathy and rational decision-making in the ultimatum game. Personality and Individual Differences 49, 451-456.
Pillutla, M.M., Murnighan, J.K., 1996. Unfairness, Anger, and Spite: Emotional Rejections of Ultimatum Offers. Organ. Behav. Hum. Decis. Process. 68, 208-224.
Price, C.J., Devlin, J.T., Moore, C.J., Morton, C., Laird, A.R., 2005. Meta-analyses of object naming: effect of baseline. Hum Brain Mapp 25, 70-82.
Raemaekers, M., Vink, M., Zandbelt, B., van Wezel, R.J., Kahn, R.S., Ramsey, N.F., 2007. Test-retest reliability of fMRI activation during prosaccades and antisaccades. Neuroimage 36, 532-542.
Reid, A.T., Hoffstaedter, F., Gong, G., Laird, A.R., Fox, P., Evans, A.C., Amunts, K., Eickhoff, S.B., 2017. A seed-based cross-modal comparison of brain connectivity measures. Brain Struct Funct 222, 1131-1151.
Ruff, C.C., Ugazio, G., Fehr, E., 2013. Changing social norm compliance with noninvasive brain stimulation. Science 342, 482-484.
Rutledge, R.B., de Berker, A.O., Espenhahn, S., Dayan, P., Dolan, R.J., 2016. The social contingency of momentary subjective well-being. Nat Commun 7, 11825.
Sanfey, A.G., 2007. Social decision-making: insights from game theory and neuroscience. Science 318,

598-602.

Sanfey, A.G., Rilling, J.K., Aronson, J.A., Nystrom, L.E., Cohen, J.D., 2003. The neural basis of economic decision-making in the Ultimatum Game. Science 300, 1755-1758.

Semmann, D., Krambeck, H.-J., Milinski, M., 2004. Strategic investment in reputation. Behavioral Ecology and Sociobiology 56.

Singer, T., Seymour, B., O'Doherty, J., Kaube, H., Dolan, R.J., Frith, C.D., 2004. Empathy for pain involves the affective but not sensory components of pain. Science 303, 1157-1162.

Singer, T., Seymour, B., O'Doherty, J.P., Stephan, K.E., Dolan, R.J., Frith, C.D., 2006. Empathic neural responses are modulated by the perceived fairness of others. Nature 439, 466-469.

Spitzer, M., Fischbacher, U., Herrnberger, B., Gron, G., Fehr, E., 2007. The neural signature of social norm compliance. Neuron 56, 185-196.

Tabibnia, G., Satpute, A.B., Lieberman, M.D., 2008. The sunny side of fairness: preference for fairness activates reward circuitry (and disregarding unfairness activates self-control circuitry). Psychological science 19, 339-347.

Turkeltaub, P.E., Eden, G.F., Jones, K.M., Zeffiro, T.A., 2002. Meta-analysis of the functional neuroanatomy of single-word reading: method and validation. Neuroimage 16, 765-780.

Turkeltaub, P.E., Eickhoff, S.B., Laird, A.R., Fox, M., Wiener, M., Fox, P., 2012. Minimizing within-experiment and within-group effects in activation likelihood estimation meta-analyses. Human brain mapping 33, 1-13.

Tzourio-Mazoyer, N., Landeau, B., Papathanassiou, D., Crivello, F., Etard, O., Delcroix, N., Mazoyer, B., Joliot, M., 2002. Automated anatomical labeling of activations in SPM using a macroscopic anatomical parcellation of the MNI MRI single-subject brain. Neuroimage 15, 273-289.

van den Bos, W., van Dijk, E., Westenberg, M., Rombouts, S.A., Crone, E.A., 2009. What motivates repayment? Neural correlates of reciprocity in the Trust Game. Social cognitive and affective neuroscience 4, 294-304.

van den Bos, W., van Dijk, E., Westenberg, M., Rombouts, S.A., Crone, E.A., 2011. Changing brains, changing perspectives: the neurocognitive development of reciprocity. Psychological science 22, 60-70.

Wager, T.D., Lindquist, M., Kaplan, L., 2007. Meta-analysis of functional neuroimaging data: current and future directions. Social cognitive and affective neuroscience 2, 150-158.

Wang, J., Fan, L., Wang, Y., Xu, W., Jiang, T., Fox, P.T., Eickhoff, S.B., Yu, C., Jiang, T., 2015. Determination of the posterior boundary of Wernicke's area based on multimodal connectivity profiles. Hum Brain Mapp 36, 1908-1924.

Wicker, B., Keysers, C., Plailly, J., Royet, J.P., Gallese, V., Rizzolatti, G., 2003. Both of us disgusted in My Insula: The common neural basis of seeing and feeling disgust. Neuron 40, 655-664.

Xiang, T., Lohrenz, T., Montague, P.R., 2013. Computational substrates of norms and their violations during social exchange. J Neurosci 33, 1099-1108a.

Yu, R., Calder, A.J., Mobbs, D., 2014. Overlapping and distinct representations of advantageous and disadvantageous inequality. Human Brain Mapping 35, 3290-3301.

Zamir, S., 2001. Rationality and Emotions in Ultimatum Bargaining. Annales d'Économie et de Statistique 61, 1-31.

Zheng, L., Wang, Q., Cheng, X., Li, L., Yang, G., Sun, L., Ling, X., Guo, X., 2016. Perceived reputation of others modulates empathic neural responses. Exp Brain Res 234, 125-132.

Figures

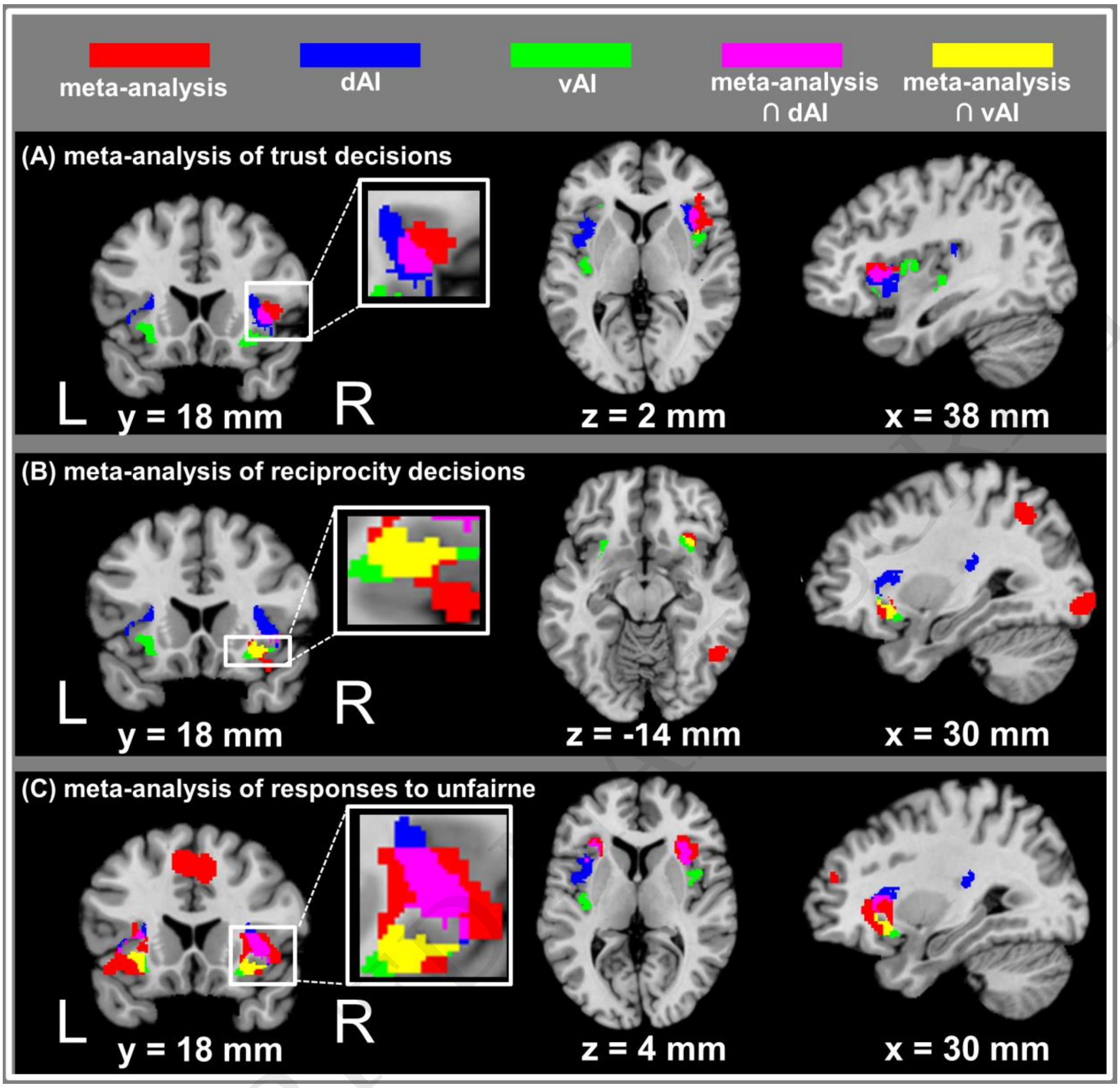

Figure 1. ALE meta-analysis results. Consistently activated regions for decisions to trust (A), decisions to reciprocate (B), and decisions to reject unfair offers (C). The corresponding overlaps with dAI and vAI were derived from Kurth et al. (2010). L, left; R, right; dAI, dorsal anterior insula; vAI, ventral anterior insula; ∩, conjunction. Meta-analysis results are illustrated in red, dAI in blue, vAI in green, the conjunction between meta-analysis results and dAI in pink and the conjunction between meta-analysis results and vAI in yellow.

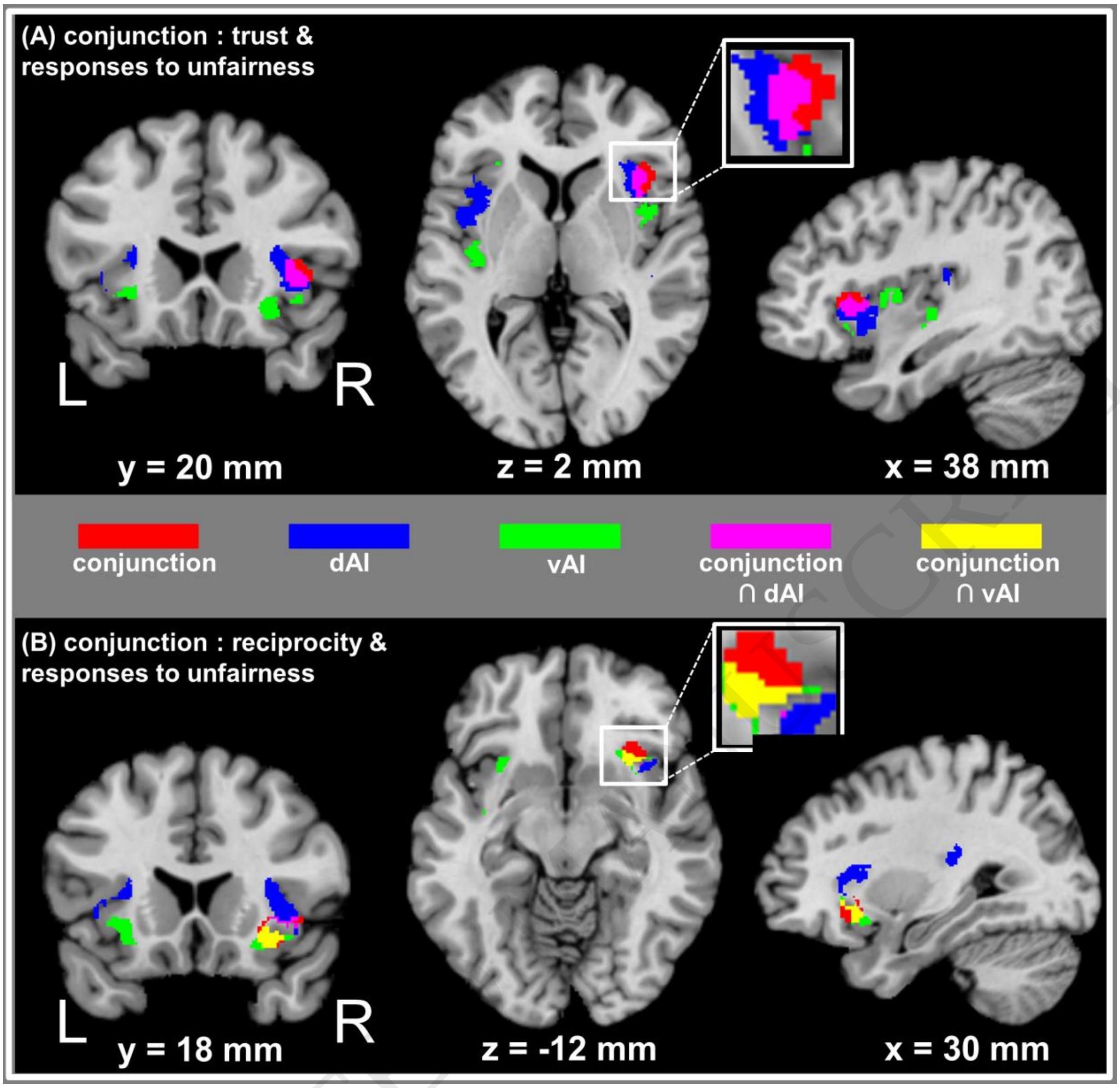

Figure 2. Conjunction analysis for common regions in the trust and ultimatum game. Conjunction between trust and response to unfairness was identified in the dAI (A), whereas conjunction between reciprocity and response to unfairness was identified in the vAI (B). The dAI and the vAI were derived from Kurth et al. (2010). L, left; R, right; dAI, dorsal anterior insula; vAI, ventral anterior insula. Conjunction results are illustrated in red, dAI in blue, vAI in green, the conjunction between meta-analysis results and dAI in pink and the conjunction between meta-analysis results and vAI in yellow.

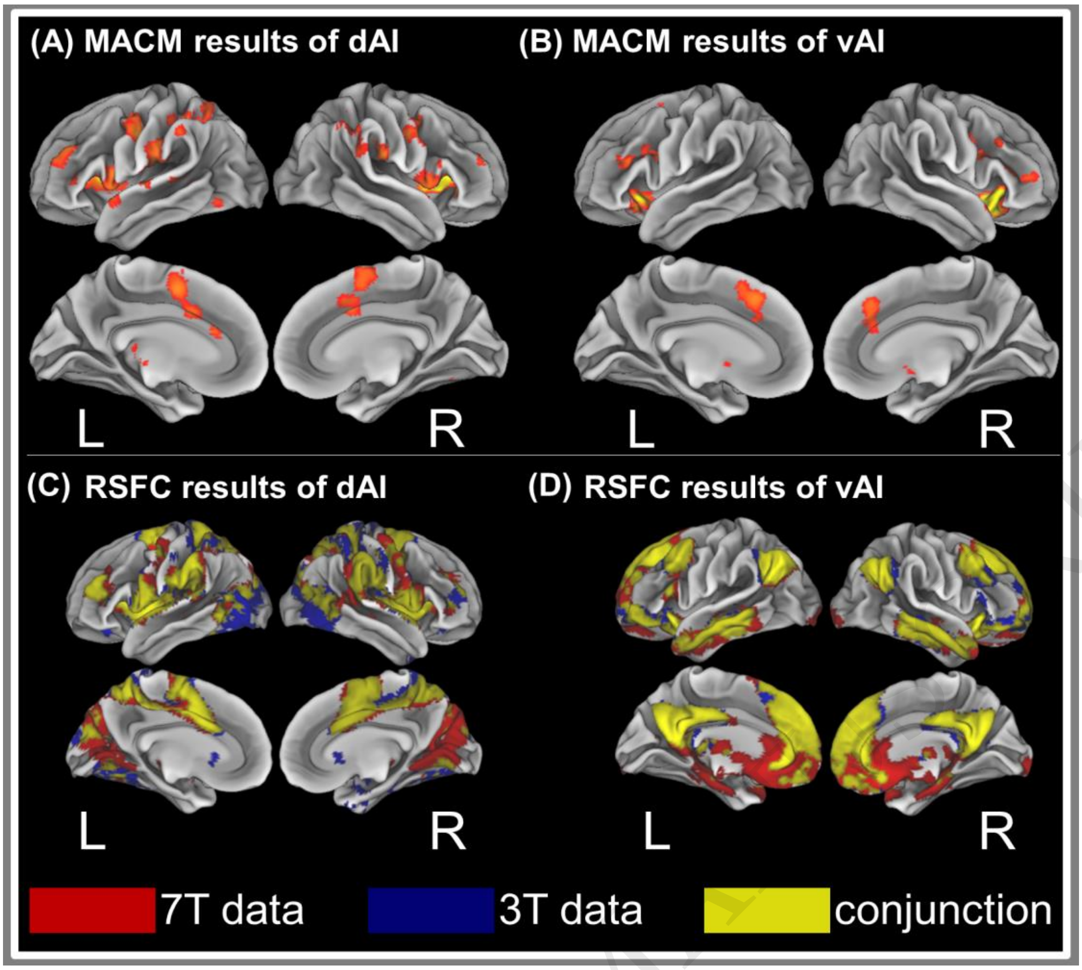

Figure 3. Task-based (MACM) and task-free (RSFC) connectivity analysis results. (A) Connectivity patterns of the dAI based on MACM analyses. (B) Connectivity patterns of the vAI based on MACM analyses. (C) Conjunction of RSFC results between dAI connectivity patterns revealed by the 7 T and 3 T dataset. (D) Conjunction of RSFC results between vAI connectivity patterns revealed by the 7 T and 3 T dataset. L, left; R, right; dAI, dorsal anterior insula; vAI, ventral anterior insula; MCAM, meta-analytic connectivity mapping; RSFC, resting-state functional connectivity; T, Tesla. RSFC connectivity from the 7 T dataset is depicted in red, from the 3 T dataset in blue, overlaps are illustrated in yellow.

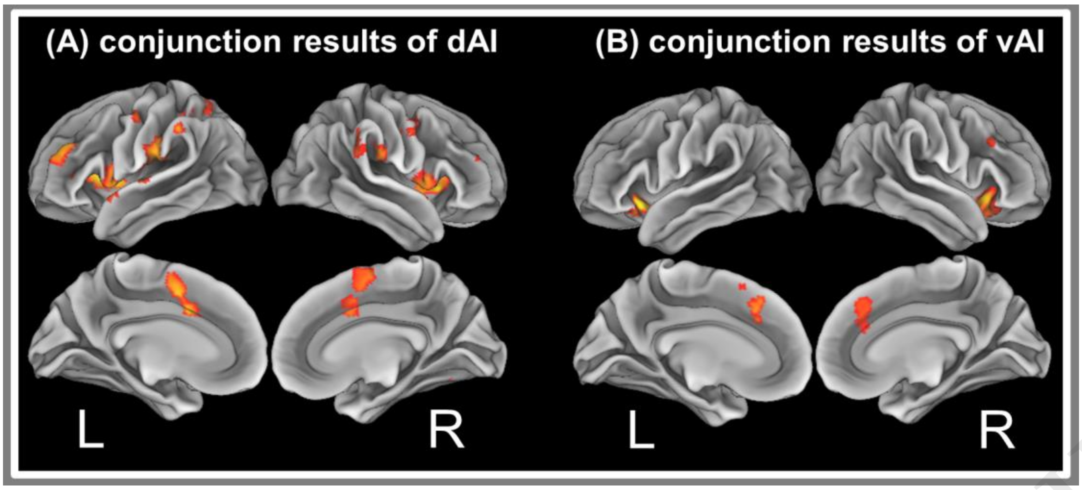

Figure 4. Conjunction analyses of MACM and RSFC analysis results. Conjunction of MACM and RSFC results (A) for dAI and (B) for vAI. L, left; R, right; dAI, dorsal anterior insula; vAI, ventral anterior insula.

Table 1. ALE meta-analysis results for regions in TG and UG.

Brain Regions	**BA**	**MNI Coordinates (mm)**			**Z score**	**Cluster Size (voxels)**
		x	y	z		
Trust in one-shot TG						
R dorsal anterior insula	45	40	20	2	5.42	179
Trust in iterative TG						
L nucleus accumbens		-2	2	-6	4.08	92
Reciprocity in iterative TG						
R ventral anterior insula	47	32	20	-8	4.54	171
R inferior temporal gyrus	37 (FG4)	54	-56	-18	4.61	188
R inferior parietal lobule	7 (hIP3)	32	-60	46	5.13	147
R inferior occipital gyrus	18 (hOc3v)	30	-94	-8	4.88	113
Rejection of unfair offers in one-shot UG						
R anterior insula	47	34	24	-4	7.08	634
L anterior insula	47	-30	22	0	5.83	521
middle cingulate gyrus	32	-4	16	46	6.49	748
R middle frontal gyrus	46	40	34	28	4.70	88
R middle frontal gyrus	46	36	50	16	5.09	84

BA, Brodmann area; anatomical assignment based on the Anatomy toolbox in parentheses; L, left; R, right; ALE, activation likelihood estimation; TG, trust game; UG, ultimatum game; MNI, Montreal Neurological Institute.

Table 2. MACM results for dorsal and ventral anterior insula.

Brain Regions	BA	MNI Coordinates (mm)			Z score	Cluster Size (voxels)
		x	y	z		
dorsal anterior insula						
L cerebellum	-	-20	-62	-20	3.20	117
R cerebellum	-	26	-66	-16	2.79	112
L middle occipital gyrus	-	-42	-68	-10	1.94	11
L putamen/inferior frontal gyrus	13	-24	8	2	8.13	1688
R insula/inferior frontal gyrus	13/47	38	10	-2	8.13	1606
L thalamus	-	-16	-14	12	3.05	334
R thalamus	-	16	-10	8	3.24	91
L supramarginal gyrus	40	-52	-22	24	3.60	478
L middle frontal gyrus	10	-44	52	8	2.07	11
L middle frontal gyrus	10	-36	40	32	3.45	193
R middle frontal gyrus	10	34	58	16	2.07	9
R inferior parietal lobule	40	56	-28	28	3.45	377
anterior cingulate gyrus	24/32	-4	28	20	2.74	16
R middle frontal gyrus	10/46	42	50	24	2.17	24
R precentral gyrus	6	54	-2	38	3.49	386
L precentral gyrus	6	-48	0	30	1.75	5
middle cingulate gyrus	6/32	-10	4	52	3.94	898
L superior parietal gyrus	7	-20	-68	40	2.11	38
L middle frontal gyrus	6	-50	-8	40	5.73	575
L inferior parietal lobule	40	-60	-40	40	2.61	14
L inferior parietal lobule	7/40	-36	-44	50	3.24	253
ventral anterior insula						
L cerebellum	-	-26	-68	-30	2.31	5
L cerebellum	-	-36	-70	-24	1.77	7
R ventral anterior insula	47	34	16	-18	8.13	1175
L ventral anterior insula	47/13	-34	18	-12	8.13	631
L middle occipital gyrus	37	-52	-64	-12	2.08	10
L brainstem	-	-6	-30	-10	2.27	14
L caudate	-	-6	4	-4	3.35	225
R middle frontal gyrus	10	36	50	8	2.34	39
R inferior frontal gyrus	46	52	40	16	3.28	109
L inferior frontal gyrus	46	-52	34	16	1.86	8

R inferior frontal gyrus	46	-36	30	20	2.88	70
R precental gyrus	9	38	2	28	2.75	102
L inferior frontal gyrus	9	-38	10	24	2.75	70
supplementary motor area	8	-6	26	46	3.78	459
L middle frontal gyrus	9	-52	22	30	2.32	27
R middle frontal gyrus	9	52	22	34	3.41	114
L dorsomedial frontal gyrus	9	-12	28	32	2.04	12
R angular	7	30	-68	46	2.05	26
R middle frontal gyrus	6	30	10	50	2.32	29
L superior frontal gyrus	6	-28	8	54	2.30	35

BA, Brodmann area; L, left; R, right; ALE, activation likelihood estimation.

Table 3. RSFC results for dorsal and ventral anterior insula.

Brain Regions	BA	MNI Coordinates (mm)			T score	Cluster Size (voxels)
		x	y	z		
Dorsal anterior insula						
3T data						
R inferior frontal gyrus/anterior insula extending to middle cingulate gyrus, middle frontal gyrus, putamen, middle temporal gyrus, thalamus, inferior parietal lobule, supramarginal and fusiform gyrus.	45	40	18	2	36.48	23585
R middle frontal gyrus	46	36	46	32	6.89	970
R caudate		16	26	0	5.84	229
R fusiform	20	38	-30	-24	5.86	75
R inferior temporal gyrus	36	36	0	-42	4.80	139
R cerebellum	(Lobule VIII)	18	-68	-46	5.47	179
R cerebellum	(Lobule VIII)	16	-54	-52	5.18	298
L inferior frontal gyrus/anterior insula extending to putamen, thalamus, middle frontal gyrus, inferior parietal lobule, and superior temporal and supramarginal gyrus.		-34	12	4	10.18	7559
L middle frontal gyrus	11 (Fo3)	-24	36	-12	6.56	170
L precentral gyrus		-46	-6	52	4.78	89
L cerebellum/middle temporal gyrus	(Lobule VI/ FG4)	-36	-48	-26	6.78	4682
L cerebellum	(Lobule VIII)	-20	-70	-46	6.17	1048
7T data						
R anterior insula extending to putamen, thalamus, middle cingulate gyrus, middle frontal gyrus, middle temporal gyrus, inferior parietal lobule, supramarginal gyrus, and middle occipital and fusiform gyrus.	44	42	14	0	17.98	56091
R middle frontal gyrus	46	32	40	24	8.93	963

Ventral anterior insula						
3T data						
R anterior insula extending to medial frontal gyrus, middle cingulate gyrus, rectus gyrus, and temporal pole.	47	32	20	-10	36.56	18752
middle cingulate gyrus	23	-8	-38	34	8.90	3853
R inferior frontal gyrus	45	54	24	8	4.96	52
R hippocampus		24	-26	-8	6.53	105
R angular		56	-56	34	10.14	2539
R caudate		14	8	14	8.01	192
R middle temporal gyrus		66	-30	-10	9.01	2833
R cerebellum		6	-54	-46	7.83	641
L hippocampus		-24	-24	-10	5.15	79
L angular gyrus	39 (PGa)	-42	-60	38	10.79	2843
L caudate		-14	16	6	5.25	71
L middle temporal gyrus	21	-64	-36	-4	8.40	2378
L cerebellum	(Lobule VIIa crus1)	-18	-88	-28	7.90	3058
7T data						
R anterior insula extending to medial frontal gyrus, middle cingulate gyrus, rectus gyrus, putamen, thalamus, and temporal pole.	47	32	18	-8	17.13	42434
R cuneus	18 (hOc1)	22	-98	-2	5.20	396
R cerebellum	(Lobule VIIa crus1)	28	-84	-34	6.80	883
L inferior frontal gyrus	45	-54	22	12	6.00	229
L angular gyrus	39 (PGa)	-42	-60	32	12.72	2746
L cerebellum	(Lobule VIIa crus1)	-16	-88	-28	6.70	1695
L cerebellum	(Lobule IX)	-6	-54	-40	5.12	221

BA, Brodmann area; anatomical assignment based on the Anatomy toolbox in parentheses; L, left; R, right; RSFC, resting-state functional connectivity; MNI, Montreal Neurological Institute.

Table 4. Conjunction analysis of MACM and RSFC results for dorsal and ventral anterior insula.

Brain Regions	**BA**	**MNI Coordinates (mm)**			**Z score**	**Cluster Size (voxels)**
		x	y	z		
dorsal anterior insula						
L cerebellum	-	-24	-62	-24	8.56	93
R cerebellum	-	24	-66	-18	6.30	59
L dorsal anterior insula/inferior frontal gyrus	13	-32	16	8	13.67	1012
R dorsal anterior insula/inferior frontal gyrus	13	40	18	2	36.48	1043
L inferior parietal lobule	40	-60	-36	26	11.80	382
L middle frontal gyrus	10	-32	40	28	9.31	182
R inferior parietal lobule	40	60	-34	34	13.05	245
R middle frontal gyrus	10	40	50	24	4.60	8
R precentral gyrus	6	46	-2	40	9.34	179
dorsal cingulate gyrus	6/32	10	8	42	12.03	697
L inferior parietal lobule	40	-58	-38	40	9.28	12
L superior parietal lobule	7	-22	-52	48	5.82	59
L postcentral gyrus	4	-46	-10	52	5.99	38
L middle frontal gyrus	6	-24	-8	58	7.04	83
L inferior parietal lobule	40	-30	-46	52	5.79	13
ventral anterior insula						
R inferior frontal gyrus/anterior insula	47	32	20	-10	36.56	555
R inferior frontal gyrus/anterior insula	47	-30	18	-10	12.62	249
L caudate	-	-8	8	4	6.70	17
R caudate	-	10	10	4	6.14	21
supplementary motor area	8/32	6	38	28	10.47	306
R inferior frontal gyrus	46	46	24	34	7.19	42
L anterior cingulate gyrus	9	-8	30	34	7.12	7
R middle frontal gyrus	6	36	10	52	5.84	12

BA, Brodmann area; anatomical assignment based on the Anatomy toolbox in parentheses; L, left; R, right; RSFC, resting-state functional connectivity; MNI, Montreal Neurological Institute.